Entangled and colloidally stable microcrystalline cellulose matrices in controlled drug release

Yujiao Dong[1], Heli Paukkonen[2], Wenwen Fang[1], Eero Kontturi[1], Timo Laaksonen[2,3], Päivi Laaksonen*[1]

[1]Department of Bioproducts and Biosystems (BIO[2]), PO Box 16300, FI-00076 Aalto University, Finland, [2]Division of Pharmaceutical Biosciences, University of Helsinki, PO Box 56, 00014, Finland, [3]Department of Chemistry and Bioengineering, PO Box 541, 33101 Tampere University of Technology, Finland.

Contact details of the corresponding author: E-mail: paivi.laaksonen@aalto.fi, Telephone: +358 50 460 2611

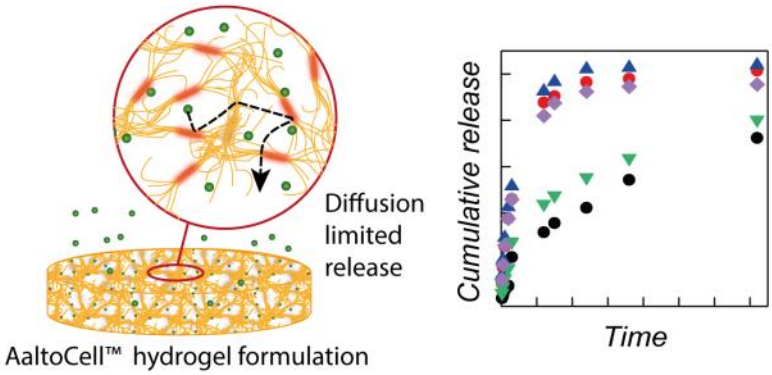

Graphical abstract

Abstract

Drug release from a new type of matrix material consisting of partially fibrillated microcrystalline cellulose was investigated. A mechanical treatment of novel AaltoCell™ cellulose microcrystals caused partial opening of the nanofibrillary structure of the cellulose particles and entanglement of individual particles led into formation of an elastic network of microcrystalline cellulose. The rheological properties of the stable hydrogel-like materials were characterised by shear rheometry. Model compounds metronidazole and lysozyme were

successfully employed in drug release experiments carried out by delignified (bleached) and lignin-containing matrices. The viscosity as well as the lignin-content played a role in the release dynamics of the drugs. Microcrystalline AaltoCell™ was proven as high-performing material for diffusion controlled release of the chosen model compounds and can be seen as a safe and economical alternative for novel matrix materials such as nanocellulose or cellulose derivatives.

Keywords: Controlled release; Cellulose hydrogel; Microcrystalline cellulose; Diffusion-limited release

1. Introduction

Cellulose is the principal structural ingredient of all plants and its use in materials applications ranges from paper and textiles to food and cosmetics. Cellulose-based materials are also abundantly utilised within the pharmaceutical realm because of their renewability, low cost, biodegradability, low toxicity and good biocompatibility. In particular, a hydrolysed, micron-sized form of pure cellulose called microcrystalline cellulose (MCC) is frequently applied as a direct compression excipient in tablet manufacturing.[1–4] MCC has good mechanical properties, and it can be used as a gelling agent[5] as well as a binder.[6,7] In particular, it is considered as one of the preferred binders in tablet production via direct compression. In addition, MCC is self-disintegrating, which can be exploited together with superdisintegrants to enhance fast dissolution of the formulation. MCC has been used in e.g. as a dispersant for spray-dried drug nanocrystals.[8] MCC is also useful in stabilizing suspensions where the stabilization is usually achieved by viscosity modification[4,9] or steric hindrance.[10,11]

In this paper, we report the use of MCC as a stand-alone drug release matrix. Previously, this has not attracted much attention, even though e.g. Dan et al. have shown that MCC/CMCS

mixtures can been used in spray-drying to both stabilize and disperse drug nanocrystals.[9] Despite this study and the afore mentioned numerous applications of MCC in pharmaceutical dosage forms, MCC as a single-component drug releasing matrix at high MCC concentrations has not been studied. The lack of preceding studies may stem from the non-porous nature of standard MCC, thus impairing its ability to sustain the drug release in the first place. Therefore, we have taken advantage of a newly introduced MCC grade dubbed AaltoCell™, prepared under scalable conditions that never allow the cellulose matrix to dry, resulting in a more porous, water-swollen MCC grade.[12] In addition, the preparation method itself for AaltoCell™ is environmentally more benign than the other processes that produce MCC. As such, AaltoCell™ presents an altogether new cellulosic product whose properties and performance in a vast number of applications are likely to differ from those of other cellulosic grades. To systematically investigate the fundamentals of the AaltoCell™ drug release system, we have employed two distinct grades: one containing lignin (amorphous polyphenol in plant cell walls) and the other delignified, mainly consisting of cellulose, representing the grade more akin to conventional MCC. Aside the release profiles of metronidazole and lysozyme, rheological properties of both dispersions were scrutinised to back up our fundamental approach. It turned out that AaltoCell™ could well provide a cheaper and more feasible alternative to nanofibrillar cellulose, which has recently been put forward as a strong candidate for a drug release medium.[13–17]

2. Material and methods

2.1. Preparation of microcrystalline cellulose

Undried microcrystalline cellulose, AaltoCell™ was prepared from white (bleached) and brown (unbleached) fibres according to an earlier protocol by Vanhatalo *et al.*[12] A flow chart presenting the processing steps is shown in Figure 1 A. For simplicity, the resulting as-prepared AaltoCell™ from bleached fibres is referred here as to MCC. MCC was processed further by

diluting it with water to 12 w-% consistency. MCC-water mixture was treated mechanically with dispersioniser equipment (Omega® 60 Economic Dispersionizer, Netzsch). The processing was carried out at 700 bars pressure while keeping the cellulose/water slurry temperature under 80 °C. To obtain a gel-like material, the MCC-water mixture was passed three times through the dispersioniser. The mechanical treatment was carried out for both bleached and unbleached grades of MCC and these are referred to here as MCC-Dispersed (MCC-D) and MCC-Lignin (MCC-L), respectively. Bleaching is a typical way of delignifying cellulose and it actually changes its colour form brown to white (see Figure 1 B-C). Total amount of lignin, including the acid soluble and insoluble parts, of the unbleached MCC-L was measured according to the NREL standard.[18] The lignin contents in MCC-L was 6.3 % of the weight. Avicel® PH-101 (Merck, Germany), was used as a reference material in the rheology experiments.

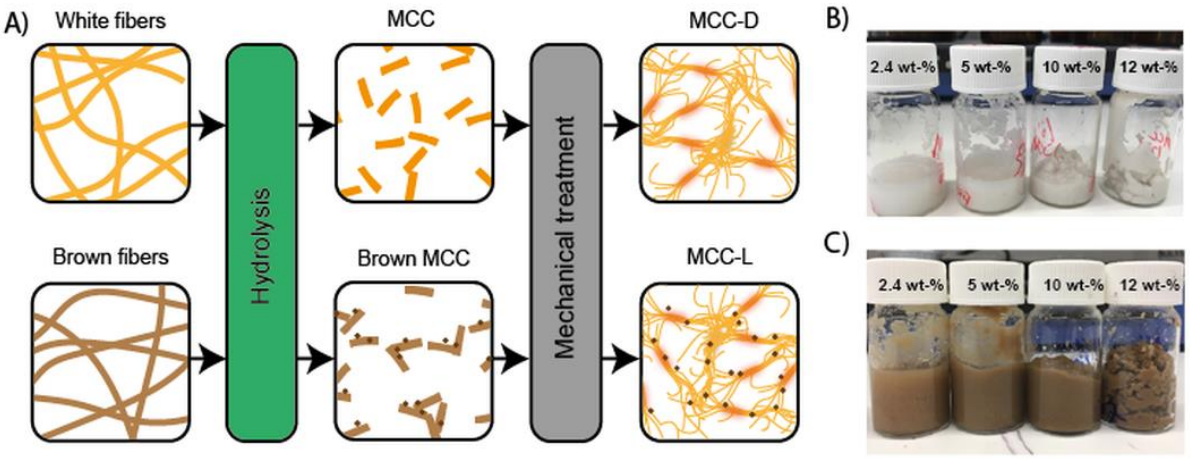

Figure 1. Preparation of MCC. A) Microcrystalline cellulose was prepared by hydrolysis from bleached cellulose fibers and from unbleached brown fibers. The mechanical treatment after hydrolysis is able to disperse the cellulose into gel-like material. B) Mechanically dispersed MCC-D samples at 2.4, 5, 10 and 12 wt-%. C) Mechanically dispersed lignin-containing MCC-L samples at 2.4, 5, 10 and 12 wt-%.

2.2. Conductometric titration for charge determination

The pH of the MCC suspension was adjusted to 2 with 0.1 M HCl and the solution was stirred for 30 min. 0.3 g of material (dry weight) was mixed with 500 mL of degassed milli-Q water with 0.5 mL of 0.5 mol dm^{-3} NaCl and 1 mL of HCl at 0.1 mol dm^{-3}. The titration was conducted with a 0.1 mol dm^{-3} NaOH solution at 0.04 ml min^{-1} titration velocity (751 GPD Titrino, Metrohm).

2.3. Drug formulations

Metronidazole (Analytical standard, Sigma-Aldrich, China) and lysozyme (Premium quality, Roche, Germany) were applied as the model drug compounds. The preparation of the MCC/drug formulations was carried out by mixing the drug powder to the 12 wt-% MCC hydrogel. The drug content was fixed to 1 wt-% of the original amount of cellulose in the samples. A manual mixing procedure was carried out by pressing the sample several times between two syringes attached by short tubing. This process was recently developed for the mixing of nanocellulose suspensions and is described in detail elsewhere. [19]

2.4. Scanning electron microscopy

The morphology of the different MCC grades was characterised by scanning electron microscopy (SEM). The samples were prepared by drop-casting a diluted MCC suspensions on silicon wafer, which was let dry in ambient conditions. The samples were sputtered with a thin layer of gold/platinum (Emitech K950X/K350, Quorum Technologies Ltd, UK) before imaging to prevent the charging of the samples. The coated samples were imaged using a field emission scanning electron microscope (Sigma VP FE-SEM, Zeiss, Germany) under the acceleration voltage of 1.5 keV.

2.5. Oscillatory shear rheometry

The rheological properties of the different MCC grades were studied by oscillatory shear rheometry (AR-G2 Magnetic Bearing Rheometer, TA Instruments, USA). The samples were studied in a parallel 20 mm diameter steel plate geometry with 1 mm gap. The temperature was set to 22 ˚C during the experiments (AWC100 Compact Recirculating Cooler, Julabo, Germany). The results were analysed with TA data analysis software.

The rheological properties of the different MCC grades were investigated by oscillatory stress sweeps and viscosity tests. In the oscillatory stress sweep, the elastic and viscotic moduli *G*' and *G*'' were measured as a function of the oscillatory stress over the range of 0.01 Pa to 100 Pa, while the frequency was kept at 1 Hz. The viscosity of the samples was measured as a function of the shear rate ranging from 0.01 to 1000 s^{-1} in a period of 5 min. All measurements were performed in triplicate and the results are presented as an average of the three measurements. The error bars represent the standard deviation of the repeats.

2.6. Drug release experiments

The drug release studies were performed with disc-shaped molds that were filled with 1.11 g of 12 wt-% MCC, MCC-D and MCC-L dispersions containing 1 wt-% of metronidazole or lysozyme. The disc molds were placed in 150 ml amber glass vials and the vials were filled to a final volume of 70 ml with pH 7.4 phosphate buffered saline. During the experiment, the dispersions remained fixed in the molds without any swelling and the surface area exposed to the release buffer remained at constant size of 1.33 cm^2. The temperature was kept at 37 °C and the vials were under constant magnetic stirring (400 rpm) on top of a multi-position magnetic stirrer (IKA RT10, IKA-Werke GmbH & Co KG, Germany). 1.5 ml samples were collected at 0.5 h, 1 h, 2 h, 4 h, 6 h, 24 h, 30 h, 48 h from the vessels and replaced with fresh buffer. Both model compounds were stable under the experimental conditions. All experiments were done in triplicate.

Diffusion coefficients (*D*) were used to quantitatively describe the diffusion controlled drug release. The dispersions were assumed to fulfill the prerequisite characteristics of slab geometry monolithic solutions where the initial drug concentration does not exceed drug solubility in the matrix.[20] Both drugs were incorporated into the dispersions at 1 wt-%, which corresponds to 10 mg ml^{-1}. The condition for monolithic solution was fulfilled as MZ has an aqueous solubility of 10.5 mg ml^{-1} [21,22] and the solubility of LZ exceeds 10 mg ml^{-1} in aqueous environment.[23,24] Therefore, the unsteady-state form of Fick's second law of diffusion with early values of time, when $0 < M_t/M_\infty < 0.6$, could be used with slab geometry for the calculations of diffusion coefficients:[20]

$$\frac{M_t}{M_\infty} = 4\left(\frac{Dt}{\pi L^2}\right)^{\frac{1}{2}} \quad (1)$$

where M_t and M_∞ denote the cumulative amounts of drug released at time t and infinite time ∞; *D* is the diffusion coefficient of the drug within the matrix system; *L* represents the thickness (1 cm) of the dispersion. *D* was obtained from fitting the data of M_t/M_∞ at selected time points. The physicochemical properties of model compounds are summarised in Table 1.

Table 1. Physicochemical properties of MZ and LZ.

Compound	Molecular weight (g mol^{-1})	Solubility (mg ml^{-1})	pK$_a$ / pI	Charge at pH 7.0	Hydrodynamic diameter (nm)
MZ	171	10.5 *,**	2.38 [25]	ø	
LZ	1.47×10^4	>10 [26]	11.1 [23]	+	~ 3.7 [24]

*at 25 °C [21], ** at pH 7 [22]

1.7 Quantification of model compounds from *in vitro* release samples

The quantification of MZ and LZ from drug release samples was performed by UV-Vis spectrophotometry (Cary 50 UV-vis, Varian Inc. USA). The absorbance was measured in 1 cm

cell at 320 nm for MZ and 280 nm for LZ against buffer as the blank. Calibration curves with squared correlation coefficients above 0.99 ($R^2 > 0.99$) were established between 3 – 35 µg ml^{-1} and 2.5 – 30 µg ml^{-1} for MZ and LZ respectively. The calibration curves for each drug are presented in Figure S1. All measurements were done in triplicate.

3. Results

3.1. Morphology and charge of MCC

The morphology of the different MCC types was studied by SEM. Images of the drop-casted MCC, MCC-D and MCC-L obtained at different magnifications are presented in Figure 2. The as-prepared MCC contains fairly large particles that appear to be fragments of their source material, *i.e.*, cellulosic fibres. However, the close-up image (Figure 2B) reveals that the sample contains a large amount of finer fibrillar elements and their pieces. The samples that had been treated mechanically, appear to consist mostly of small fibre fragments and fine fibrillar elements that have spread and formed a layer on the sample surface. Overall, the particle size distributions of all never-dried AaltoCell™ samples are qualitatively different from traditional MCC grades where the particle size has generally been controlled with spray drying.[27]

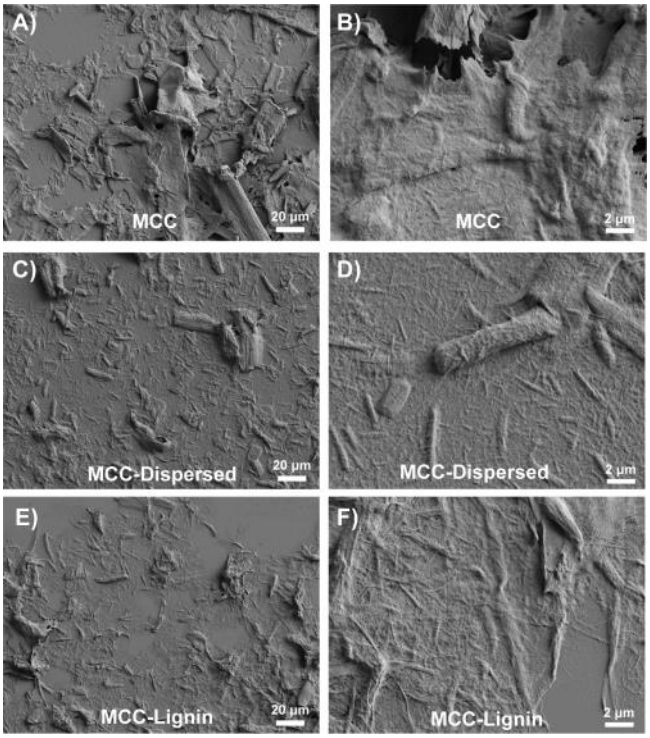

Figure 2. SEM images of as-prepared MCC A), B), mechanically dispersed MCC C), D) and lignin-containing MCC E) and F).

The results of the conductometric titration are summarised in Table 2. The charge is presented as the molar amount of acidic groups per a gram of pulp and was reasonably low for all the samples. The charges of MCC and MCC-D were similar, indicating to unchanged chemical composition after the mechanical treatment. The lignin-containing MCC-L had slightly higher negative charge.

Table 2. The result of the conductometric titration (n = 3).

Sample	**mmol COOH / g pulp**
MCC	0.03 ± 0.01
MCC-D	0.03 ± 0.01
MCC-L	0.07 ± 0.02

3.2. Rheological properties of the MCC

Gel-forming ability of the different MCC grades and a commercial reference Avicel at 10 wt-% was studied by measuring the elastic moduli of the hydrogels (Figure 3A). The highest elastic moduli were measured for the mechanically dispersed MCC-L and MCC-D, having values near 100 kPa and 10 kPa, respectively. The modulus of the as-prepared MCC was at the kPa range, whereas the Avicel suspension had the lowest values at the Pa range. The stress sweeps showed a constant modulus until the stress exceeded the yield point of the gel and the moduli dropped significantly. For dispersed MCC-D and MCC-L the yield point was above the maximum applied stress 100 Pa and could not thus be accurately defined, but for the MCC and Avicel the yielding occurred near 30 Pa and 2 Pa respectively.

The stress sweep measurements were carried out similarly for the MCC-D at different concentrations (Figure 3B). The elastic modulus decreased from tens of kPa to the 100 Pa level when decreasing the concentration from 12 wt-% to 2.4 wt-%. The yield point of the hydrogels decreased in the order of descending concentration. The values of the loss moduli *G*'' were typically 1 decade smaller than *G*' for each sample (see Figure S1).

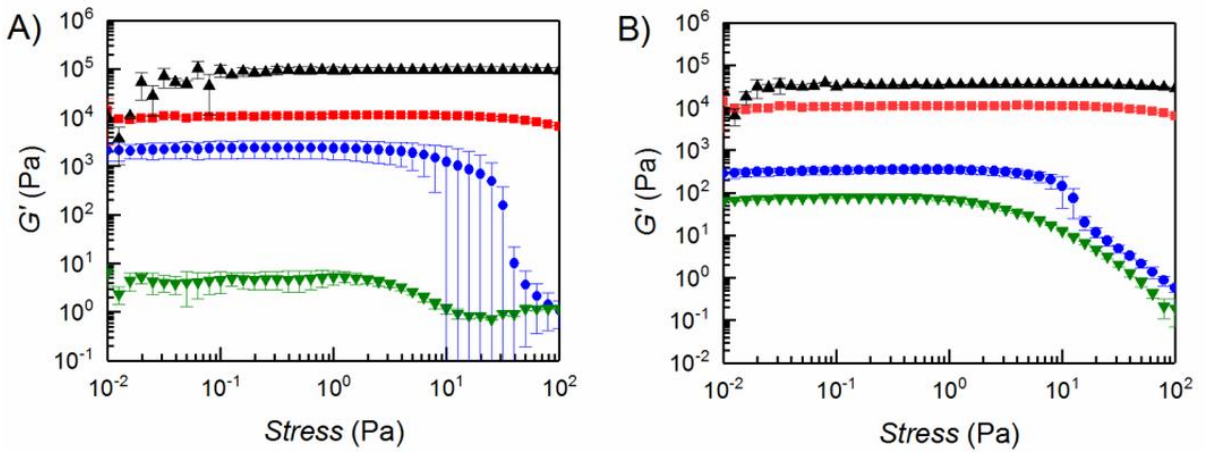

Figure 3. A) Storage modulus as a function of the oscillatory stress measured for MCC-L (black up-pointing triangles), MCC-D (red squares), MCC (blue dots) and Avicel (green down-pointing triangles) at 10 wt-%. B) Storage modulus as a function of the oscillatory stress

measured for MCC-D at 12 wt-% (black up-pointing triangles), 10 wt-% (red squares), 5 wt-% (blue dots) and 2.4 wt-% (green down-pointing triangles).

The viscosity of the MCC samples as well as the Avicel at 10 wt-% were measured as a function of the shear rate (Figure 4A). All the samples showed a shear thinning behaviour with rather linear dependence between viscosity and shear rate. The descendent order of the viscosity for the different MCC grades was MCC-L, MCC-D, MCC and Avicel. The viscosity of a dilution series of MCC-D is presented in Figure 4B. In all dilutions, the MCC-D behaved as shear thinning fluid, having a linear dependency between viscosity and concentration. Viscosities of the 12 wt-% MCC-L hydrogels before and after blending in the drug molecules were measured (see Figure S2). MCC-L formulations appeared 10 times more viscous than the other formulations.

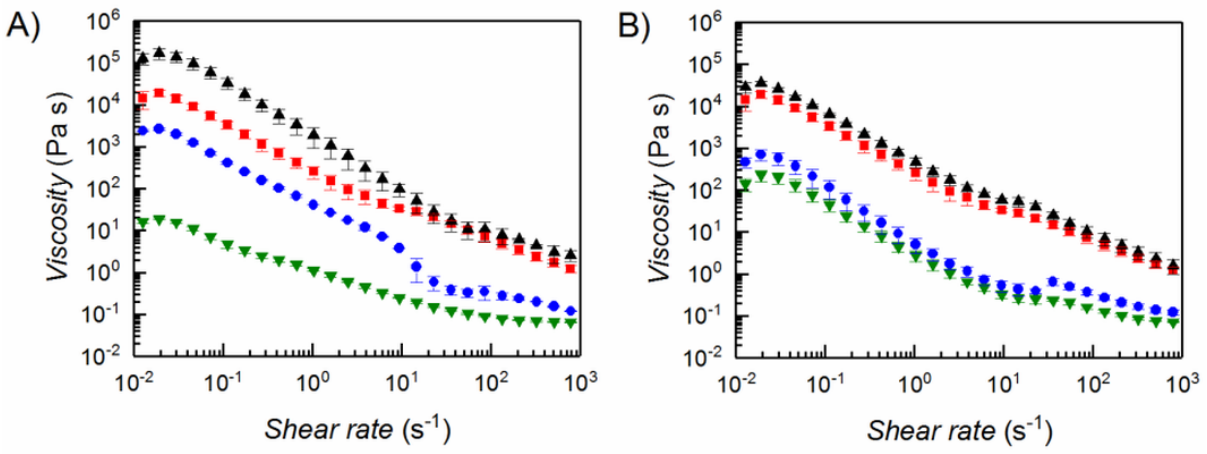

Figure 4. A) Viscosity as a function of the shear rate measured for MCC-L (black up-pointing triangles), MCC-D (red squares), MCC (blue dots) and Avicel (green down-pointing triangles) at 10 wt-%. B) Viscosity as a function of the shear rate measured for MCC-D at 12 wt-% (black up-pointing triangles), 10 wt-% (red squares), 5 wt-% (blue dots) and 2.4 wt-% (green down-pointing triangles).

3.3. Drug release experiments

The release studies were performed in order to evaluate the applicability of 12 wt-% AaltoCell™ matrices in controlled drug release applications. We further aimed to test whether the mechanical treatment or lignin content had an impact on drug release properties. MZ was selected primarily due to its low molecular weight (171 g mol^{-1}) and neutral charge at pH 7.4, whereas LZ represents a high molecular weight (1.47 x 10^4 g mol^{-1}) protein compound that has a cationic charge at pH 7.4. MZ and LZ were completely dissolved in MCC, MCC-D and MCC-L matrices and therefore the formulations were by definition monolithic solutions. The cumulative release of drug compounds from the different MCC matrices is presented in Figure 5. The experimental release profiles of MZ and LZ were fitted to a theoretical model based on Fickian diffusion equations for early drug release, i.e. $0 < M_t/M_\infty < 0.6$. The experimental and theoretical values were very close, indicating diffusion-controlled release. It was clearly observed that the drug release for MZ was faster from all matrices, whereas sustained release profiles were observed for LZ.

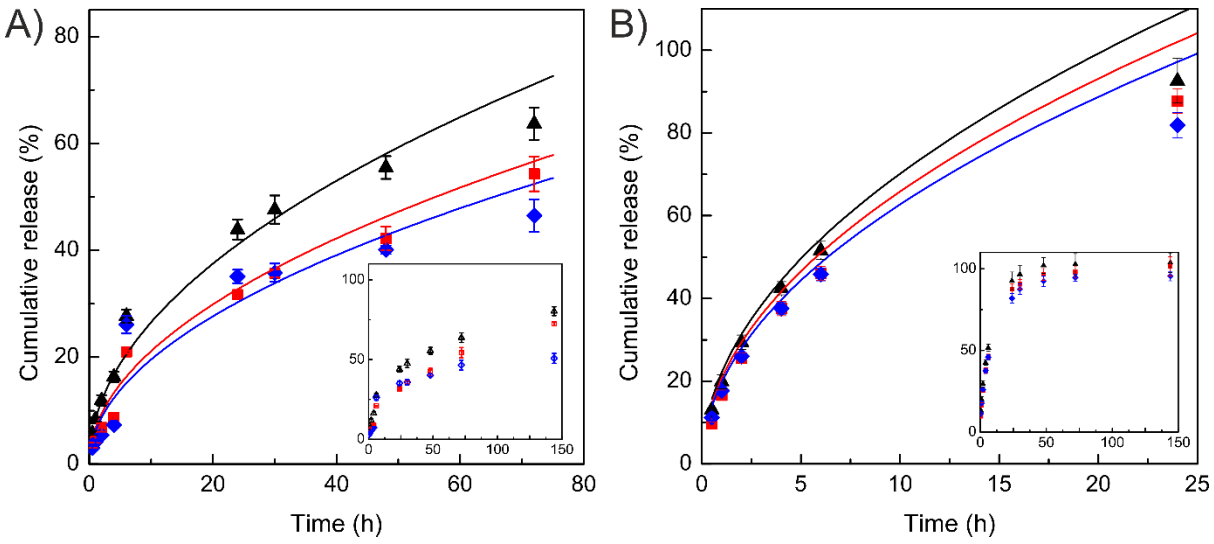

Figure 5. Cumulative release profiles for A) lysozyme and B) metronidazole from the different matrices. Experimental results are presented as symbols (n = 3 ± stdev) whereas the solid lines

are the fits to the theoretical prediction of the unsteady-state form of Fick's second law of diffusion with early values of time when $0 < M_t/M_\infty < 0.6$. The MCC matrices were MCC-D (black triangles), MCC (red squares) and MCC-L (blue diamonds). Insets: The measured release data of the whole experiments with the same time and release fraction ranges for both experiments.

For MZ and LZ, the drug release rates from different MCC matrices occurred from the fastest to the slowest in the order of MCC-D > MCC > MCC-L. However, for MZ the differences in the cumulative drug release profiles from different matrices were relatively small. From MCC-D 52 % was released at 6 h and 100 % was reached at 48 h. From both, MCC and MCC-L matrix, 46 % was released at 6 h, whereas 100 % from MCC and 96 % from MCC-L was reached at 144 h. For LZ, however the overall cumulative drug release % from all matrices was lower. From MCC-D 56 % was released at 48 h and 80 % release was reached at 48 h. From both, MCC and MCC-L matrix, close to 40 % was released at 48 h, whereas cumulative release of 72 % from MCC and 51 % from MCC-L was reached at 144 h.

The well-established Fickian model was used to calculate diffusion coefficients for MZ and LZ inside the MCC matrices (eq. 1, materials and methods). The results are presented in Table 3. In all matrices, the diffusion coefficient of MZ near ten-fold in comparison to LZ. For LZ there was a nearly two-fold difference in the diffusion coefficient measured in MCC-D and MCC-L indicating that lignin content prolonged further the diffusion of LZ.

Table 3. Diffusion coefficients for MZ and LZ in the different MCC matrices.

Matrix	D_{MZ} **(×10^{-8} cm^2 s^{-1})**	D_{LZ} **(×10^{-8} cm^2 s^{-1})**
MCC	237	24
MCC–D	269	38
MCC–L	215	21

4. Discussion

Mechanical treatment clearly decreased the particle size of MCC and after the treatment the majority of the needle-like cellulose crystals had dimensions below 10 µm (Figure 2). The particles appear to be bundles of partly dispersed microfibrils with a hairy appearance. The fine fibrils pointing out from the MCC particles had a strong ability to form a continuous film upon drying, which implies rather strong interfibrillar interactions, expected for cellulosic fibrils with high surface area. Thus, the mechanical treatment resulted in cellulose microparticles having fibrillary surfaces. This property renders dispersed AaltoCell™ particles quite different from the existing commercial MCC grades where such fibrillation of the surface has not been reported. A previous report found that in materials similar to the unbleached MCC-L, lignin is enriched on the particle surfaces, thus forming a thin coating on the particles, which may affect the mechanical properties and wetting of the particles.[28] However, lignin did not have a marked effect in the mechanical treatment that was carried out at liquid state and the resulting MCC-L had very similar features with the treated MCC-D (Figures 2-4).

Based on their higher viscosity as well as higher elasticity, the ability to form a gel was significantly greater for the mechanically dispersed samples MCC –D and MCC -L, due to the opened fibrillar structure. The accessible surface area of the MCC particles most probably increased in the mechanical treatment and the nanofibrils pointing out from the microparticles could strongly interact with other particles through entanglement. These interparticular interactions are a likely reason for the elastic gel-like properties, distinguishing the dispersed grades from the undispersed MCC and Avicel that behaved as unstable suspensions. Sedimentation of the MCC suspension caused instability in the rheometry measurements, which was observed, for instance as the large variation in the *G*' value shown in Figure 3 A. The entanglement of the nanofibrils enhanced also the strength of the gel against large shear forces since the yield point was much higher for the dispersed samples.

The MCC matrices did not exhibit any swelling during the release studies and therefore diffusion was the main release mechanism for the model compounds. The diffusion coefficient is inversely proportional to the size of the molecules and therefore faster diffusion of the smaller MZ was anticipated. In literature, a solution diffusivity value of 104×10^{-8} cm^2 s^{-1} has been reported for LZ[29] whereas for a small molecule having molar mass below 500 g mol^{-1}, the solution diffusivity is typically higher, 600 - 900×10^{-8} cm^2 s^{-1}.[30] Diffusion coefficients for both LZ and MZ inside all tested AaltoCell™ matrices (see Table 2) were significantly smaller that the corresponding literature values for free diffusion in solutions, which indicates that the AaltoCell™ hydrogels could be used to efficiently control the diffusion of both large and small molecular size compounds and this has great potential for controlled drug release applications. The charge of the different celluloses could be considered low, thus the electrostatic interactions between the drug and the matrix did not have a substantial contribution to the drug release rate. The lignin-containing MCC-L had slightly more negative charge than the other grades, which may have led into some attractive interaction between LZ, which has a positive charge at pH 7.4.

The different AaltoCell™ matrices also had different apparent viscosities which are reflected on the release profiles. The viscosities of the different drug formulations from the highest to the lowest were in the order MCC-L > MCC-D > MCC (Figure S2). MCC-L had a 10-fold higher viscosity than the other formulations and expectedly the release rates of both MZ and LZ were the slowest from this matrix. The hydrogel has a non-homogeneous structure consisting of water reservoirs that are trapped in solid porous matrix and connected via water capillaries. The drug that is dissolved in the water phase can diffuse in the water but does not cross the solid barriers. Due to its larger size, the physical entrapment of LZ in the highly viscous AaltoCell™ matrices likely allowed less free motion for diffusion than for smaller MZ, which explains the slower diffusion and release. Quantitative comparison of the apparent

hydrogel viscosity and the viscosity that the molecule experiences is not straightforward and thus directly linking the apparent viscosity to the release profiles is not discussed further.

The prolonged drug release from the lignin containing matrix MCC-L was especially significant for LZ. Lignin has an amorphous and slightly hydrophobic structure due to multiple aromatic groups and it is possible that hydrophobic interactions between lignin and lysozyme protein further prolonged the release from the MCC-L matrix.[31] Only a handful of studies have explored lignin matrices in controlled drug release applications and typically the amorphous lignin structure has been exploited for drug encapsulation via hydrophobic interactions.[32] In our study, lignin was an integral part of the MCC-L matrix and may have decreased the release rate through non-specific adsorption of LZ. Hydrophobic surfaces attract the hydrophobic amino acids within proteins and in close contact, this attraction is able to affect the protein conformation and to lead in to non-specific adhesion of the protein.[33] Non-specific adhesion may be observed for instance, as lowered enzyme activity. Lysozyme has been shown to enhance the catalytic degradation of lignocellulosic materials when hydrolysis has been carried out with a mixture of cellulase and lysozyme.[34] As protein with no enzymatic activity, lysozyme could enhance the hydrolysis only by adhering to the lignin-rich areas thus reducing the non-specific adsorption of the cellulase. Another study has shown that proteins easily adsorb on lignin surfaces but may still remain hydrated which can be essential for proteins to maintain their structure and functionality.[35] For considering controlled release of a delicate drug molecule, such as peptide or a full protein, it is important that the interactions between the matrix and the molecule do not become too great to avoid a possible loss in the bioactivity of the drug.

In a previous study, 3 wt-% and 6.5 wt-% carboxylated anionic nanofibrillated cellulose (ANFC) hydrogels were studied as the drug release matrix. The obtained control for MZ release from 12 wt-% AaltoCell™ matrices were higher as the diffusion coefficient from

aforementioned ANFC hydrogels were close to the level of free diffusion.[19] On the contrary, the release control achieved for LZ was higher with the ANFC hydrogels as the diffusion appeared ten-fold slower than in the present study. Due to multiple carboxylic groups, these particular ANFC fibrils had an anionic surface charge 15-30 times higher than in the AaltoCell samples in this study. For reference, ANFC was been reported to have a charge density of 1.03 mmol g^{-1} of fibers[19]. The anionic charges provide binding sites for the positively charged LZ and can therefore stabilise its attachment in the matrix. The structure of the ANFC hydrogel also differs from AaltoCell™ as it consists of a highly entangled nanofibrillar network, whereas the AaltoCell™ hydrogels are basically interconnected microcrystal networks.[19,36] Despite the differences, MCC-based matrices could be used in similar controlled release applications as ANFC hydrogels. Benefits of Aaltocell™ grades include the fact that it is easily dispersed with the mechanical treatment and great colloidal stability could be obtained for MCC-D and MCC-L. As these grades are manufactured from never dried pulp there should be no irreversible aggregation of cellulose microfibrils upon drying (hornification effect) and the porosity of the materials remains high. Furthermore, the adjustment of different MCC solid concentrations is possible, effect of which on drug release properties could be evaluated in the future.

Viscosity of the hydrogel matrix and its physical interactions with the drug molecules were the most significant factors that controlled the drug release rates of encapsulated model compounds MZ and LZ. Chemical interactions between model compounds and the MCC matrices such as hydrophobic interactions, hydrogen bonding and electrostatic forces were also present, but are not seen as major reasons behind the sustained release rates. Additionally, the availability of free water molecules and water capillary interconnections in the different MCC matrices generally affects the diffusion rate of molecules and these also played a role for the obtained diffusion coefficients.

5. Conclusions

Functional, yet affordable gel-like drug release matrices based on microcrystalline cellulose were investigated. The materials chosen for the study were based on non-derivatised never-dried cellulose that, after a mechanical treatment, were able to form a gel. All gels remained stable under physiological conditions and worked well as a matrix for the controlled release of metronidazole and lysozyme. The mechanical treatment was able to fibrillate the MCC partly, resulting in micron-sized particles with nanofibrillar surfaces that could form interparticular interactions through entanglement and form a network of microparticles. Thanks to these interactions, the MCC, which usually forms a suspension, became a gel. Bleached and unbleached variants of the gels had different features, especially in the release of lysozyme that was more sustained in the lignin-containing MCC-L hydrogel. A hierarchical cellulose matrix combining features of both micron and nanoscale cellulose is a new matrix material candidate for drug release applications.

6. Acknowledgements

The financial support from Academy of Finland (Grant No. 258114) as well as the Academy of Finland Center of Excellence Program, especially the Center of Excellence in Molecular Engineering of Biosynthetic Hybrid Materials (HYBER) is gratefully acknowledged. This work made use of the facilities at the Aalto University Nanomicroscopy Center (Aalto-NMC) premises.

7. Appendices

Supplementary material containing complimentary rheological data including G'' measurements of the different MCC grades and MCC-D dilution series as well as viscosity measurement of the drug formulations.

8. References

(1) Klemm, D.; Heublein, B.; Fink, H.-P.; Bohn, A. Cellulose: Fascinating Biopolymer and Sustainable Raw Material. *Angew. Chemie Int. Ed.* **2005**, *44* (22), 3358–3393.

(2) Rowe, R. C.; Sheskey, P. J.; Weller, P. J. *Handbook of Pharmaceutical Excipients*, 4th editio.; Rowe, R. C., Sheskey, P. J., Weller, P. J., Eds.; Pharmaceutical Press: London, 2003.

(3) Trache, D.; Hussin, M. H.; Hui Chuin, C. T.; Sabar, S.; Fazita, M. R. N.; Taiwo, O. F. A.; Hassan, T. M.; Haafiz, M. K. M. Microcrystalline Cellulose: Isolation, Characterization and Bio-Composites Application—A Review. *Int. J. Biol. Macromol.* **2016**, *93*, 789–804.

(4) Nsor-Atindana, J.; Chen, M.; Goff, H. D.; Zhong, F.; Sharif, H. R.; Li, Y. Functionality and Nutritional Aspects of Microcrystalline Cellulose in Food. *Carbohydr. Polym.* **2017**, *172*, 159–174.

(5) Kleinebudde, P. The Crystallite-Gel-Model for Microcrystalline Cellulose in Wet-Granulation, Extrusion, and Spheronization. *Pharm. Res.* **1997**, *14* (6), 804–809.

(6) Bolhuis, G. K.; Anthony Armstrong, N. Excipients for Direct Compaction—an Update. *Pharm. Dev. Technol.* **2006**, *11* (1), 111–124.

(7) Badawy, S. I. F.; Gray, D. B.; Hussain, M. A. A Study on the Effect of Wet Granulation on Microcrystalline Cellulose Particle Structure and Performance. *Pharm. Res.* **2006**, *23* (3), 634–640.

(8) Mostafa, H. F.; Ibrahim, M. A.; Sakr, A. Development and Optimization of Dextromethorphan Hydrobromide Oral Disintegrating Tablets: Effect of Formulation and Process Variables. *Pharm. Dev. Technol.* **2013**, *18* (2), 454–463.

(9) Dan, J.; Ma, Y.; Yue, P.; Xie, Y.; Zheng, Q.; Hu, P.; Zhu, W.; Yang, M. Microcrystalline Cellulose-Carboxymethyl Cellulose Sodium as an Effective Dispersant for Drug Nanocrystals: A Case Study. *Carbohydr. Polym.* **2016**, *136*, 499–506.

(10) Kalashnikova, I.; Bizot, H.; Cathala, B.; Capron, I. New Pickering Emulsions Stabilized by Bacterial Cellulose Nanocrystals. *Langmuir* **2011**, *27* (12), 7471–7479.

(11) Oza, K. P.; Frank, S. G. Drug Release From Emulsions Stabilized by Colloidal Macrocrystalline Cellulose. *J. Dispers. Sci. Technol.* **1989**, *10* (2), 187–210.

(12) Vanhatalo, K. M.; Dahl, O. P. Effect of Mild Acid Hydrolysis Parameters on Properties of Microcrystalline Cellulose. *BIORESOURCES* **2014**, *9* (3), 4729–4740.

(13) Valo, H.; Arola, S.; Laaksonen, P.; Torkkeli, M.; Peltonen, L.; Linder, M. B.; Serimaa, R.; Kuga, S.; Hirvonen, J.; Laaksonen, T. Drug Release from Nanoparticles Embedded in Four Different Nanofibrillar Cellulose Aerogels. *Eur. J. Pharm. Sci.* **2013**, *50* (1), 69–77.

(14) Kolakovic, R.; Laaksonen, T.; Peltonen, L.; Laukkanen, A.; Hirvonen, J. Spray-Dried Nanofibrillar Cellulose Microparticles for Sustained Drug Release. *Int. J. Pharm.*

2012, *430* (1), 47–55.

(15) Kolakovic, R.; Peltonen, L.; Laukkanen, A.; Hirvonen, J.; Laaksonen, T. Nanofibrillar Cellulose Films for Controlled Drug Delivery. *Eur. J. Pharm. Biopharm.* **2012**, *82* (2), 308–315.

(16) Zografi, G.; Kontny, M. J. The Interactions of Water with Cellulose- and Starch-Derived Pharmaceutical Excipients. *Pharm. Res.* **1986**, *3* (4), 187–194.

(17) Paukkonen, H.; Ukkonen, A.; Szilvay, G.; Yliperttula, M.; Laaksonen, T. Hydrophobin-Nanofibrillated Cellulose Stabilized Emulsions for Encapsulation and Release of BCS Class II Drugs. *Eur. J. Pharm. Sci.* **2017**, *100*, 238–248.

(18) Sluiter, A.; Hames, B.; Ruiz, R.; Scarlata, C.; Sluiter, J.; Templeton, D.; Crocker, D. *Determination of Structural Carbohydrates and Lignin in Biomass*; Golden, 2008.

(19) Paukkonen, H.; Kunnari, M.; Laurén, P.; Hakkarainen, T.; Auvinen, V.-V.; Oksanen, T.; Koivuniemi, R.; Yliperttula, M.; Laaksonen, T. Nanofibrillar Cellulose Hydrogels and Reconstructed Hydrogels as Matrices for Controlled Drug Release. *Int. J. Pharm.* **2017**, *532* (1), 269–280.

(20) Siepmann, J.; Siepmann, F. Modeling of Diffusion Controlled Drug Delivery. *J. Control. Release* **2012**, *161* (2), 351–362.

(21) Kim, H.; Lee, Y.; Yoo, H.; Kim, J.; Kong, H.; Yoon, J.-H.; Jung, Y.; Kim, Y. M. Synthesis and Evaluation of Sulfate Conjugated Metronidazole as a Colon-Specific Prodrug of Metronidazole. *J. Drug Target.* **2012**, *20* (3), 255–263.

(22) Wu, Y.; Fassihi, R. Stability of Metronidazole, Tetracycline HCl and Famotidine Alone and in Combination. *Int. J. Pharm.* **2005**, *290* (1), 1–13.

(23) Fritz, M.; Radmacher, M.; Cleveland, J. P.; Allersma, M. W.; Stewart, R. J.; Gieselmann, R.; Janmey, P.; Schmidt, C. F.; Hansma, P. K. Imaging Globular and Filamentous Proteins in Physiological Buffer Solutions with Tapping Mode Atomic Force Microscopy. *Langmuir* **1995**, *11* (9), 3529–3535.

(24) Szymańska, A.; Ślósarek, G. Light Scattering Studies of Hydration and Structural Transformations of Lysozyme. *Acta Phys. Pol. A* **2012**, *121* (3), 694–698.

(25) Zhou, C.; Jin, Y.; Kenseth, J. R.; Stella, M.; Wehmeyer, K. R.; Heineman, W. R. Rapid PKa Estimation Using Vacuum-Assisted Multiplexed Capillary Electrophoresis (VAMCE) with Ultraviolet Detection. *J. Pharm. Sci.* **2018**, *94* (3), 576–589.

(26) Howard, S. B.; Twigg, P. J.; Baird, J. K.; Meehan, E. J. The Solubility of Hen Egg-White Lysozyme. *J. Cryst. Growth* **1988**, *90* (1), 94–104.

(27) Peyre, J.; Paakkonen, T.; Reza, M.; Kontturi, E. Simultaneous Preparation of Cellulose Nanocrystals and Micron-Sized Porous Colloidal Particles of Cellulose by TEMPO-Mediated Oxidation. *Green Chem.* **2015**, *17* (2), 808–811.

(28) Vanhatalo, K.; Maximova, N.; Perander, A.-M.; Johansson, L.-S.; Haimi, E.; Dahl, O. Comparison of Conventional and Lignin-Rich Microcrystalline Cellulose. *BIORESOURCES* **2016**, *11* (2), 4037–4054.

(29) Koutsopoulos, S.; Unsworth, L. D.; Nagai, Y.; Zhang, S. Controlled Release of Functional Proteins through Designer Self-Assembling Peptide Nanofiber Hydrogel

Scaffold. *Proc. Natl. Acad. Sci.* **2009**, *106* (12), 4623 LP-4628.

(30) Hazel, J. R.; Sidell, B. D. A Method for the Determination of Diffusion Coefficients for Small Molecules in Aqueous Solution. *Anal. Biochem.* **1987**, *166* (2), 335–341.

(31) Hatakeyama, H.; Hatakeyama, T. Lignin Structure, Properties, and Applications BT - Biopolymers: Lignin, Proteins, Bioactive Nanocomposites; Abe, A., Dusek, K., Kobayashi, S., Eds.; Springer Berlin Heidelberg: Berlin, Heidelberg, 2010; pp 1–63.

(32) Chowdhury, M. A. The Controlled Release of Bioactive Compounds from Lignin and Lignin-Based Biopolymer Matrices. *Int. J. Biol. Macromol.* **2014**, *65*, 136–147.

(33) Roach, P.; Farrar, D.; Perry, C. C. Interpretation of Protein Adsorption: Surface-Induced Conformational Changes. *J. Am. Chem. Soc.* **2005**, *127* (22), 8168–8173.

(34) Toyosawa, Y.; Ikeo, M.; Taneda, D.; Okino, S. Quantitative Analysis of Adsorption and Desorption Behavior of Individual Cellulase Components during the Hydrolysis of Lignocellulosic Biomass with the Addition of Lysozyme. *Bioresour. Technol.* **2017**, *234*, 150–157.

(35) Salas, C.; Rojas, O. J.; Lucia, L. A.; Hubbe, M. A.; Genzer, J. On the Surface Interactions of Proteins with Lignin. *ACS Appl. Mater. Interfaces* **2013**, *5* (1), 199–206.

(36) Saito, T.; Kimura, S.; Nishiyama, Y.; Isogai, A. Cellulose Nanofibers Prepared by TEMPO-Mediated Oxidation of Native Cellulose. *Biomacromolecules* **2007**, *8* (8), 2485–2491.